

Fundamental Limits to Radiative Heat Transfer: The Limited Role of Nanostructuring in the Near-Field

Prashanth S. Venkataram, Sean Molesky, Weiliang Jin, and Alejandro W. Rodriguez
Department of Electrical Engineering, Princeton University, Princeton, New Jersey 08544, USA



(Received 5 July 2019; published 9 January 2020)

In a previous Letter, we derived fundamental limits to radiative heat transfer applicable in near- through far-field regimes, based on the choice of material susceptibilities and bounding surfaces enclosing arbitrarily shaped objects; the limits exploit algebraic properties of Maxwell's equations and fundamental principles such as electromagnetic reciprocity and passivity. In this Letter, we apply these bounds to two different geometric configurations of interest, namely dipolar particles or extended structures of infinite area in the near field of one another. We find that while near-field radiative heat transfer between dipolar particles can saturate purely geometric “Landauer” limits, bounds on extended structures cannot, instead growing very slowly with respect to a material response figure of merit (an “inverse resistivity” for metals) due to the deleterious effects of multiple scattering between bodies. While nanostructuring can produce infrared resonances, it is generally unable to further enhance the resonant energy transfer spectrum beyond what is practically achieved by planar media at the surface polariton condition.

DOI: [10.1103/PhysRevLett.124.013904](https://doi.org/10.1103/PhysRevLett.124.013904)

Radiative heat transfer (RHT) between two bodies may be written as a frequency integral of the form

$$P = \int_0^\infty |\Pi(\omega, T_B) - \Pi(\omega, T_A)| \Phi(\omega) d\omega \quad (1)$$

where $\Pi(\omega, T)$ is the Planck function and $\Phi(\omega)$ a dimensionless spectrum of energy transfer. RHT between two objects sufficiently separated in space ($d \gg \hbar c/k_B T$) follows the Planck blackbody law, but in the near-field where separations are smaller than the characteristic thermal wavelength of radiation, contributions to RHT from evanescent modes often dominate, allowing $\Phi(\omega)$ to exceed the far-field blackbody limits by orders of magnitude. Moreover, because the Planck function decays exponentially with frequency, judicious choice of materials and nanostructured geometries can yield resonances in Φ at lower (especially infrared) frequencies, allowing observation of even larger integrated RHT powers [1–5]. However, after accounting for the effects of such tailoring, the degree to which the spectrum Φ at a given frequency can be enhanced remains an open question. The inability of trial-and-error explorations and optimization procedures [6,7] to saturate prior bounds on Φ based on modal analyses [8–11] or energy conservation [12] suggests that these prior bounds are too loose.

In a complementary Letter [1], we derived new bounds that simultaneously account for material and geometric constraints as well as multiple scattering effects. These bounds, valid from the near- through far-field regimes, incorporate the dependence of the optimal modal response of each object on the other while simultaneously being constrained by passivity considerations in isolation. They

depend on a general material response factor (“inverse resistivity” for metals) [12],

$$\zeta = \frac{|\chi|^2}{\text{Im}(\chi)}, \quad (2)$$

without making explicit reference to specific frequencies or dispersion models, and are domain monotonic, increasing with object volumes independently of their shapes. Consequently, our bounds are applicable at all length scales, from quasistatic to ray optics regimes, do not suffer from unphysical divergences with respect to vanishing material dissipation or object sizes [12], and can be tailored to account for specific object shapes as needed.

In this Letter, we apply the aforementioned bounds on the spectrum Φ to two situations of practical interest, comparing predictions to prior bounds based on energy conservation [12], tight only in the quasistatic regime, or Landauer-like modal summations [8–11], tight only in regimes where material dissipation effects can be ignored. Specifically, we consider limits on RHT between dipolar particles as well as extended structures of infinite area and arbitrary shapes restricted to the *near-field*: domain monotonicity means that a bound on a planar domain of infinite extent is a bound on any nanostructured geometry contained within. We find that our exact bound for dipolar particles is able to reach Landauer limits when ζ exceeds a certain threshold; in contrast, bounds that neglect the interplay between material and radiative constraints overestimate possible material enhancements, diverging with increasing ζ . For extended structures, we find that the bound grows only weakly (logarithmically) with respect to

ζ , making the neglect of the interplay of material and geometric constraints even more apparent. Fundamentally, previous limits [12], in analogy with Kirchhoff's law [2,4], assumed that thermal fields produced within a given body in isolation can be perfectly absorbed by others in proximity, while neglecting the extent to which multiple scattering between bodies counteracts such absorption, explaining the aforementioned performance gap. Finally, we discuss practical implications and design guidelines for structures enhancing NFRHT: nanostructuring improves P by tailoring infrared resonances in Φ , but cannot significantly enhance Φ at peak values beyond that seen in resonant planar media. While our bounds apply directly to the spectrum Φ , they can be generalized to heat transfer over finite bandwidths assuming the spectrum at each frequency can be optimized independently.

General bounds.—We now briefly recapitulate the bounds on RHT between bodies A and B derived in detail in [1] and describe their salient features. These bounds are derived for bodies $p \in \{A, B\}$ with arbitrary homogeneous local isotropic susceptibilities χ_p and arbitrary shape and size. They depend on material constraints, particularly passivity (nonnegativity of far-field scattering by each object in isolation and in the presence of the other), encoded in the material response factors $\zeta_p = |\chi_p|^2 / \text{Im}(\chi_p)$, and on geometric constraints encoded in the off-diagonal vacuum Maxwell Green's function $\mathbb{G}_{BA}^{\text{vac}}$, which solves $[(c/\omega)^2 \nabla \times (\nabla \times) - \mathbb{I}] \mathbb{G}^{\text{vac}} = \mathbb{I}$. In particular, the bounds rest on the singular values $\{g_i\}$, which we term “radiative efficacies,” obtained from a singular-value decomposition,

$$\mathbb{G}_{BA}^{\text{vac}} = \sum_i g_i |\mathbf{b}_i\rangle \langle \mathbf{a}_i|, \quad (3)$$

where $|\mathbf{a}_i\rangle$ and $|\mathbf{b}_i\rangle$ are the corresponding right and left singular vectors, respectively. The radiative efficacies measure how strongly these bases are coupled by electromagnetic waves, and are domain monotonic, increasing with increasing domain volume even (surprisingly) beyond the near-field.

We list the relevant bounds in Table I. The main results of this paper rely on the upper bound Φ_{opt} , which we refer to as an “exact bound” in that it is valid from the near- through far-field regimes, though below we focus only on near-field effects. Φ_{opt} is domain monotonic in that it always increases with increasing object volumes, and this comes from the domain monotonicity of g_i . Therefore, one can choose to evaluate the bound in a domain of high symmetry enclosing the objects of interest, representing a fundamental geometric constraint in analogy and in combination with material constraints imposed by a specific choice of ζ_p . We clarify that interference and wave effects will of course be important to computing the actual spectrum Φ for two specific objects, but these effects are somewhat less immediately relevant for computing Φ_{opt} between generic domains.

TABLE I. Summary of various bounds on NFRHT limits. Φ_{opt} captures radiative and geometric constraints via the singular values $\{g_i\}$ of the vacuum Green's function $\mathbb{G}_{BA}^{\text{vac}}$, and material constraints via the response factors $\zeta_p = [|\chi_p|^2 / \text{Im}(\chi_p)]$ for $p = \{A, B\}$. Θ is the Heaviside step function. As described in the main text, restricted versions of Φ_{opt} each capture different facets of this bound.

Bound	Formula	Material factor	Bounded per channel
Φ_{opt}	$\sum_i (1/2\pi) \Theta(\zeta_A \zeta_B g_i^2 - 1) + \sum_i (2/\pi) [\zeta_A \zeta_B g_i^2 / (1 + \zeta_A \zeta_B g_i^2)^2] \Theta(1 - \zeta_A \zeta_B g_i^2)$	Yes	Yes
Φ_{qs}	$\sum_i (2/\pi) \zeta_A \zeta_B g_i^2$	Yes	No
Φ_L	$\sum_i (1/2\pi)$	No	Yes

The expression for Φ_{opt} shows that optimal heat transfer is achievable if the modes of the response of each body coincide with the modes of the *vacuum* Green's function $\mathbb{G}_{BA}^{\text{vac}}$ (whereas using the modes of the *total* Green's function \mathbb{G}_{BA} would yield Φ itself for a specific system, not a general bound on Φ). For each channel i , each term may be physically interpreted as follows. The first term $1/2\pi$, which is the maximum per-channel contribution to Φ_{opt} , corresponds to the per-channel Landauer limit [8–11, 13, 14]. A given channel i attains this only if $\zeta_A \zeta_B g_i^2 \geq 1$, meaning that while certain channels efficiently couple electromagnetic fields propagating in vacuum between the two bodies can readily saturate their Landauer limits, other channels instead require larger material response factors ζ_p for this to occur. In contrast, the total Landauer bound Φ_L assumes saturation of every channel i (the first term) regardless of material response or geometric configuration. The second term $(2/\pi) [\zeta_A \zeta_B g_i^2 / (1 + \zeta_A \zeta_B g_i^2)^2]$ never exceeds the per-channel Landauer limit of $1/2\pi$ due to material limits, and corresponds to each body attaining its maximum absorptive response in isolation for the respective incident fields $|\mathbf{a}_i\rangle$ and $|\mathbf{b}_i\rangle$ for channel i in order to satisfy passivity constraints; the numerator corresponds to the contribution from absorption of each body in isolation, while the denominator captures multiple scattering effects between bodies. Note that if material-limited contributions were to be taken over all channels, not just those for which $\zeta_A \zeta_B g_i^2 < 1$, this would represent perfect absorption by each body in isolation for *all* channels. Such a situation can arise for bodies near polaritonic resonances, so we use this as a metric for how close Φ for uniform polaritonic media in each domain can practically approach Φ_{opt} . The “quasistatic bound” Φ_{qs} accounts for material response constraints but neglects the effects of multiple scattering between bodies, so it is tight only in quasistatic systems, and its contributions per channel may be unbounded [12]. In [1], we proved that these bounds satisfy the inequalities

$$\Phi_{\text{opt}} \leq \Phi_{\text{qs}}, \Phi_L, \quad (4)$$

regardless of the particular bounding domain. Thus, we compare them for specific topologies of interest in the asymptotic near-field (nonretarded) regime.

Dipolar bodies.—We first consider NFRHT between either two dipolar particles or a dipolar particle and an extended bulk medium of infinite area and thickness [Fig. 1(a)], enclosed within spherical or semi-infinite bounding domains, as detailed in the Supplemental Material [15]. The dipolar limit implies that if V is the volume of a dipolar particle and d is the separation from the other body, then $V^{1/3}/d \ll 1$, and no higher-order particle multipoles should matter. This also implies that there are only three degrees of freedom or singular values (i.e., polarizations) and therefore three channels. In either case, we can immediately write the Landauer limit as $\Phi_L = 3/2\pi$. The asymptotic near-field (nonretarded) radiative efficacies are $g_1 = g_2 = \sqrt{\kappa}/4\pi$ and $g_3 = 2g_1$ for two dipolar domains of volumes $V_{A,B}$ and separation d with $\kappa = V_A V_B/d^6$, and $g_1 = g_2 = \sqrt{\kappa}/64\pi$ and $g_3 = \sqrt{2}g_1$ for a dipolar domain of volume V at a distance d above a semi-infinite planar bulk domain with $\kappa = V/d^3$.

In both cases, the quasistatic bound depends linearly on the product $\zeta_A \zeta_B$, which explains why for increasing material response factors (assuming fixed volumes and separations) the bound eventually crosses the Landauer limits and never saturates. By contrast, Φ_{opt} monotonically approaches Φ_L from below with increasing material response factors (e.g., small dissipation). We note that whether the dipolar volume is near another or an extended domain, the smallest two radiative efficacies are equal to each other and correspond to the two axes perpendicular to the line of separation, while the largest radiative efficacy is larger than the smaller two by different factors depending on the particular case. This dependence implies that for the Landauer bounds to be fully saturated, the optimal net response of each body cannot be isotropic, even though the underlying susceptibilities are assumed to be isotropic; the optimal dipole should instead arise for an oblate ellipsoidal shape whose aspect ratio is a

function of $g_{\text{max}}/g_{\text{min}}$, while the optimal extended structure (assuming an isotropic particle) should be textured in order to break homogeneity. However, in both cases, if the material-limited contributions $(2/\pi)[\zeta_A \zeta_B g_i^2 / (1 + \zeta_A \zeta_B g_i^2)^2]$ are used for every channel, the resulting Φ is only 10% smaller than Φ_{opt} at $\sqrt{\zeta_A \zeta_B \kappa} \approx 10$, where the dipolar particle size is comparable to the skin depth. Such a situation arises when the surface polariton condition is met, corresponding to $\text{Re}(1/\chi) = -1/2$ for a uniform planar bulk or $\text{Re}(1/\chi) = -1/3$ for an isotropic dipolar sphere. Thus, we find that given appropriate polaritonic materials, nanostructuring enhances Φ little over uniform high-symmetry structures.

Extended structures.—We now consider NFRHT between two extended structures of infinite area A separated by a distance d . In this case, there is an infinite continuum of participating channels, labeled by the two-dimensional in-plane wave vector \mathbf{k} , and the sum over channels i becomes $\sum_i \rightarrow A \iint [d^2 k / (2\pi)^2]$. Furthermore, even after normalizing to the area, the Landauer bound $\Phi_L/A = \iint (1/2\pi) [d^2 k / (2\pi)^2]$ diverges, so we do not consider it further. The remaining bounds Φ_{opt} and Φ_{qs} , after multiplying by a common factor of d^2/A , only depend on the product of material factors $\sqrt{\zeta_A \zeta_B}$ and on no other length scales in the near-field.

As we show in the supplement [15], the asymptotic near-field (nonretarded) radiative efficacies $g(\mathbf{k}) = e^{-|\mathbf{k}|d}/2$ for two planar semi-infinite bounding regions yield simple analytical forms for the bounds, with

$$\begin{aligned} \Phi_{\text{opt}} \times \frac{d^2}{A} &= \frac{1}{4\pi^2} \ln \left(1 + \frac{\zeta_A \zeta_B}{4} \right) + \frac{\Theta(\zeta_A \zeta_B - 4)}{8\pi^2} \\ &\times \left\{ \ln(\zeta_A \zeta_B) + \frac{1}{4} \left[\ln \left(\frac{\zeta_A \zeta_B}{4} \right) \right]^2 - 2 \ln \left(1 + \frac{\zeta_A \zeta_B}{4} \right) \right\}, \end{aligned} \quad (5)$$

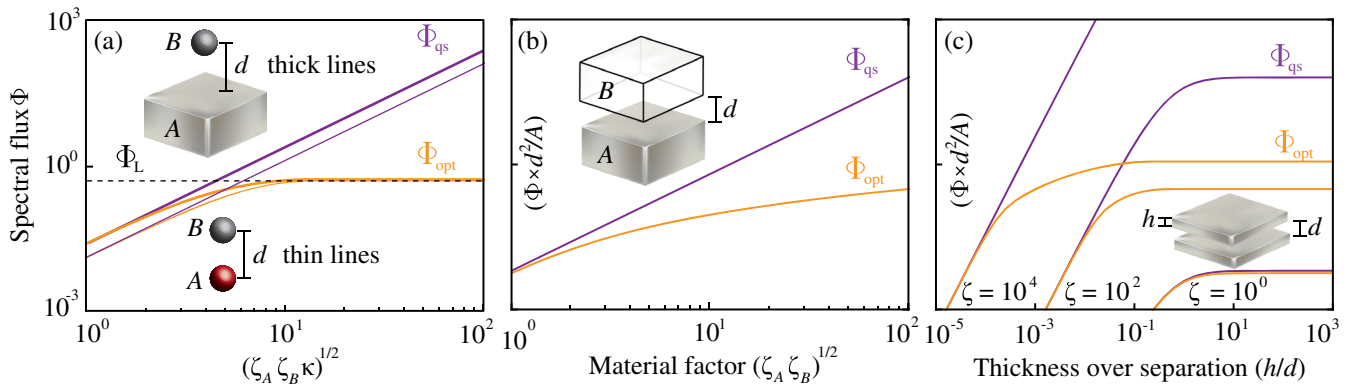


FIG. 1. Comparison of Φ_{opt} (orange) to Φ_{qs} (purple) for (a) two dipolar bodies of volumes $V_{A,B}$ (thin lines, $\kappa = V_A V_B/d^6$) or a dipolar of volume V body and an extended structure (thick lines, $\kappa = V/d^3$), (b) two extended structures of infinite thickness and area A , or (c) or two extended structures of finite thickness h . Φ_L is also shown in (a). Note that bounds between two extended structures are normalized by A/d^2 .

while $\Phi_{\text{qs}} \times d^2/A = \zeta_A \zeta_B / (16\pi^2)$. As observed in [Fig. 1(b)], both bounds converge to one another for small $\zeta_A \zeta_B$. As $\zeta_A \zeta_B$ increases, the quasistatic bounds overestimate the extent to which NFRHT can be optimized due to its simple linear dependence on $\zeta_A \zeta_B$, while the exact bound grows with respect to $\zeta_A \zeta_B$ in a much slower logarithmic fashion. Moreover, in (5), the first term represents the material-limited contributions for every channel \mathbf{k} , achievable by homogeneous isotropic planar bulk media at the surface polariton resonance condition $\text{Re}(1/\chi) = -1/2$. The correction due to progressive saturation of the Landauer bounds, given by the second term in (5), diverges (due to the divergent Φ_L) so slowly that for practically achievable ζ , Φ_{opt} is essentially achieved by planar polar dielectric bulk media. Thus, even more so than for dipolar bodies, there is very little room for enhancing Φ through nanostructuring compared to what can be achieved by planar polar dielectric media.

We also evaluate Φ_{opt} and Φ_{qs} for planar films of finite thickness h [Fig. 1(c)], where each of these bounds only depends on d and h via the common term A/d^2 and a function that depends only on $\zeta_A \zeta_B$ and the ratio h/d . Here, the radiative efficacies are $g(\mathbf{k}) = (e^{-|\mathbf{k}|d}/2)(1 - e^{-2|\mathbf{k}|h})$. We find that for thin films (compared to the separation), Φ_{opt} converges to Φ_{qs} for decreasing thickness at each value of $\zeta = \sqrt{\zeta_A \zeta_B}$, consistent with decreasing multiple scattering between bodies. However, as the thickness increases even to $h/d \approx 0.1$, each of these bounds quickly approaches its respective bulk asymptote (the limit $h/d \rightarrow \infty$). Moreover, the logarithmic scale on the plot makes clear that these asymptotic values of Φ_{qs} grow linearly with $\zeta_A \zeta_B$, whereas the corresponding growth of Φ_{opt} is logarithmic. Note that if the material-limited contributions were instead used for every channel, representing planar films of finite thickness at the surface polariton resonance condition (depending on h), the result Φ would be practically indistinguishable from Φ_{opt} . This again suggests that while reaching the exact bounds for a given thickness h would require nanoscale texturing, the bounds can be practically reached by planar films of the same thickness and appropriately chosen materials, in line with previous observations restricted to one-dimensionally periodic media [17].

Having considered bounds for generic materials with arbitrary ζ , we now turn to bounds for realistic materials of susceptibility $\chi(\omega)$ [using the corresponding definition of $\zeta(\omega)$]. In particular, we compare the power spectrum $\Phi_{\text{planar}}(\omega) \times d^2/A$ associated with identical planar films [6,12] to the exact and quasistatic bounds in Fig. 2, specifically considering gold (Au), doped silicon (Si), and silicon carbide (SiC) as representative materials. The largest heat transfer observed in specific nanostructured Au [18] and Si [7] surfaces studied in the past are also included for comparison. (We employ Drude dispersions for Au [18]

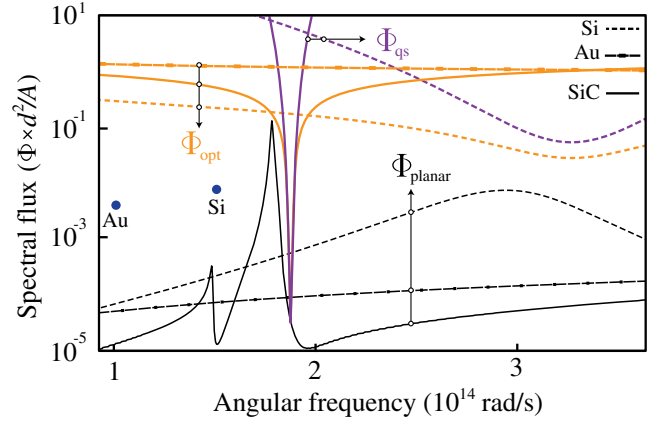


FIG. 2. Comparison of $\Phi_{\text{qs}}(\omega)$ (purple) and $\Phi_{\text{opt}}(\omega)$ (orange) for extended bodies to planar heat transfer $\Phi_{\text{planar}}(\omega)$ (black) at frequencies ω relevant to the Planck function at typical experimental temperatures, corresponding to Au (dot-dashed), doped Si (dashed), and SiC (black). Also shown with labeled dots are the maximum Φ of representative nanostructured Au [18] and doped Si [7] surfaces. Φ_{qs} for Au is several orders of magnitude above the plotted range.

and Si [7], and a phonon polaritonic dispersion for SiC [19].) In the infrared where the Planck function is considerable (at typical experimental temperatures, $T \lesssim 1000$ K), Φ_{qs} for all of these materials is significantly larger than the corresponding Φ_{opt} and is highly sensitive to material dispersion; as a specific example, the quasistatic bound for Au lies significantly above the upper limits of the plot over the entire range of frequencies shown. By contrast, the logarithmic dependence of Φ_{opt} on ζ means that it will generally be much less sensitive to changes in material dispersion except near polariton resonances, which Si and SiC feature in the infrared. We find that Φ_{planar} is consistently much smaller than either Φ_{qs} or Φ_{opt} for Au owing to the lack of infrared resonances; the Au nanostructures of [18] improve on the results for plates by two orders of magnitude, but still fall more than two orders of magnitude shy of Φ_{opt} at that frequency. The outlook is more pessimistic for polar dielectrics like doped Si or SiC. In [7], nanostructuring Si into a metasurface increases the integrated NFRHT power P by creating lower-frequency resonances in Φ . However, this does not increase the peak values of Φ above Φ_{planar} , which never reaches its bound because the dispersion of Si prohibits the planar surface plasmon resonance condition $\text{Re}(1/\chi) = -1/2$ from being reached. Meanwhile, SiC plates exhibit a power spectrum Φ_{planar} that nearly touches Φ_{opt} at two points, the smaller of which is the material resonance where the losses become so large that Φ_{opt} and Φ_{qs} coincide (as we have that shown multiple scattering between bodies becomes irrelevant for large dissipation), and the larger of which is a polaritonic resonance where Φ_{opt} is nearly constant while Φ_{qs} is larger by a factor of 50. We note that for each of

these materials at polaritonic resonances, $\Phi_{\text{planar}} \times d^2/A = (1/4\pi^2) \ln[1 + (\zeta_A \zeta_B/4)]$ is exactly the material-limited contribution to (5), which is only marginally smaller than the squared logarithmic dependence of Φ_{opt} as a whole.

Concluding remarks.—The results above suggest that apart from tailoring resonances in the infrared to improve P (especially useful for metals), nanostructuring of either dipolar or extended media cannot produce significantly better results for Φ than resonant spherical or planar objects, eventually saturating or exhibiting a logarithmic dependence on $\zeta = |\chi|^2/\text{Im}(\chi)$ in each case. At first glance, this is a surprising contrast to the success of nanostructuring in enhancing the local density of states [20]. This dichotomy can be understood as a consequence of finite-size effects: a dipole radiator does not scatter fields and hence an infinite number of modes can participate in absorption, but this cannot hold for objects of finite size.

While we have focused on NFRHT at individual resonance frequencies, our bounds can easily be extended to integrated RHT P via (1), specifically by defining $P_{\text{opt}} = \int_0^\infty |\Pi(\omega, T_B) - \Pi(\omega, T_A)| \Phi_{\text{opt}}(\omega) d\omega$ and using comparisons like Fig. 2 to guide such assessments, given that P_{opt} will depend on the material dispersion properties under consideration. Typically, P is increased by exploiting narrow resonances of bandwidth $\Delta\omega \sim \omega[\text{Im}(\chi)/|\chi|]$ in the spectrum Φ in low-loss materials, so this permits approximate bounds on the integrated heat transfer [12],

$$P_{\text{opt}} \approx \frac{\omega \text{Im}(\chi)}{|\chi|} \Phi_{\text{opt}}(\omega) |\Pi(\omega, T_B) - \Pi(\omega, T_A)|, \quad (6)$$

for two bodies of the same susceptibility χ . For dipolar bodies, Φ_{opt} reaches a maximum with respect to ζ and never diverges, while for extended structures the divergence is logarithmic. Hence, beyond a threshold, any increase in Φ_{opt} from larger material response will be accompanied by a corresponding decrease in $\Delta\omega$. This suggests that regardless of object sizes, there exists an optimal ζ maximizing P at a finite value. Further constraints could be obtained through stronger sum rules arising from frequency integration [21], the subject of future work.

Finally, we emphasize that while the above analyses focused on the near-field, which can be justified for small enough separations ($d \ll \hbar c/k_B T$), Φ_{opt} is in general finite at every length scale, whereas Φ_{qs} often diverges beyond the near-field. That said, as discussed in [1], our bounds do not explicitly include the effects of *far-field* radiative losses, which in conjunction with multiple scattering between bodies should provide even tighter bounds. Additionally, similar bounds could be derived for other problems in fluctuational electromagnetism, including fluorescence energy transfer [22] and Casimir forces [23], the subject of future work.

The authors would like to thank Riccardo Messina and Pengning Chao for helpful discussions. This work was supported by the National Science Foundation under Grants No. DMR-1454836, No. DMR 1420541, No. DGE 1148900, the Cornell Center for Materials Research MRSEC (Award No. DMR-1719875), and the Defense Advanced Research Projects Agency (DARPA) under Agreement No. HR00111820046. The views, opinions and/or findings expressed are those of the authors and should not be interpreted as representing the official views or policies of the Department of Defense or the U.S. Government.

-
- [1] S. Molesky, P. S. Venkataram, W. Jin, and A. W. Rodriguez, companion paper, Fundamental limits to radiative heat transfer: Theory, *Phys. Rev. B* **101**, 035408 (2020).
 - [2] A. I. Volokitin and B. N. J. Persson, Radiative heat transfer between nanostructures, *Phys. Rev. B* **63**, 205404 (2001).
 - [3] G. Domingues, S. Volz, K. Joulain, and J.-J. Greffet, Heat Transfer Between Two Nanoparticles Through Near Field Interaction, *Phys. Rev. Lett.* **94**, 085901 (2005).
 - [4] A. I. Volokitin and B. N. J. Persson, Near-field radiative heat transfer and noncontact friction, *Rev. Mod. Phys.* **79**, 1291 (2007).
 - [5] B. Song, Y. Ganjeh, S. Sadat, D. Thompson, A. Fiorino, V. Fernández-Hurtado, J. Feist, F.J. Garcia-Vidal, J. C. Cuevas, P. Reddy *et al.*, Enhancement of near-field radiative heat transfer using polar dielectric thin films, *Nat. Nanotechnol.* **10**, 253 (2015).
 - [6] W. Jin, R. Messina, and A. W. Rodriguez, Overcoming limits to near-field radiative heat transfer in uniform planar media through multilayer optimization, *Opt. Express* **25**, 14746 (2017).
 - [7] V. Fernández-Hurtado, F.J. García-Vidal, S. Fan, and J. C. Cuevas, Enhancing Near-Field Radiative Heat Transfer with Si-Based Metasurfaces, *Phys. Rev. Lett.* **118**, 203901 (2017).
 - [8] J. B. Pendry, Radiative exchange of heat between nanostructures, *J. Phys. Condens. Matter* **11**, 6621 (1999).
 - [9] G. Bimonte, Scattering approach to casimir forces and radiative heat transfer for nanostructured surfaces out of thermal equilibrium, *Phys. Rev. A* **80**, 042102 (2009).
 - [10] S.-A. Biehs, E. Rousseau, and J.-J. Greffet, Mesoscopic Description of Radiative Heat Transfer at the Nanoscale, *Phys. Rev. Lett.* **105**, 234301 (2010).
 - [11] P. Ben-Abdallah and K. Joulain, Fundamental limits for noncontact transfers between two bodies, *Phys. Rev. B* **82**, 121419(R) (2010).
 - [12] O. D. Miller, S. G. Johnson, and A. W. Rodriguez, Shape-Independent Limits to Near-Field Radiative Heat Transfer, *Phys. Rev. Lett.* **115**, 204302 (2015).
 - [13] S. Datta, *Electronic Transport in Mesoscopic Systems*, Cambridge Studies in Semiconductor Physics and Microelectronic Engineering (Cambridge University Press, Cambridge, England, 1995).
 - [14] J. C. Klöckner, M. Bürkle, J. C. Cuevas, and F. Pauly, Length dependence of the thermal conductance of

- alkane-based single-molecule junctions: An ab initio study, *Phys. Rev. B* **94**, 205425 (2016).
- [15] See supplemental Material at <http://link.aps.org/supplemental/10.1103/PhysRevLett.124.013904> for more details about the notation and asymptotic near-field singular values g_i for the topologies considered here; it includes Ref. [16].
- [16] L. Novotny and B. Hecht in *Principles of Nano-Optics* (Cambridge University Press, Cambridge, England, 2006), pp. 335–362.
- [17] O. D. Miller, S. G. Johnson, and A. W. Rodriguez, Effectiveness of Thin Films in Lieu of Hyperbolic Metamaterials in the Near Field, *Phys. Rev. Lett.* **112**, 157402 (2014).
- [18] R. Messina, A. Noto, B. Guizal, and M. Antezza, Radiative heat transfer between metallic gratings using fourier modal method with adaptive spatial resolution, *Phys. Rev. B* **95**, 125404 (2017).
- [19] X.-J. Hong, T.-B. Wang, D.-J. Zhang, W.-X. Liu, T.-B. Yu, Q.-H. Liao, and N.-H. Liu, The near-field radiative heat transfer between graphene/SiC/hBN multilayer structures, *Mater. Res. Express* **5**, 075002 (2018).
- [20] O. D. Miller, A. G. Polimeridis, M. T. H. Reid, C. W. Hsu, B. G. DeLacy, J. D. Joannopoulos, M. Soljačić, and S. G. Johnson, Fundamental limits to optical response in absorptive systems, *Opt. Express* **24**, 3329 (2016).
- [21] H. Shim, L. Fan, S. G. Johnson, and O. D. Miller, Fundamental Limits to Near-Field Optical Response Over Any Bandwidth, *Phys. Rev. X* **9**, 011043 (2019).
- [22] A. G. Polimeridis, M. T. H. Reid, W. Jin, S. G. Johnson, J. K. White, and A. W. Rodriguez, Fluctuating volume-current formulation of electromagnetic fluctuations in inhomogeneous media: Incandescence and luminescence in arbitrary geometries, *Phys. Rev. B* **92**, 134202 (2015).
- [23] O. Kenneth and I. Klich, Opposites Attract: A Theorem about the Casimir Force, *Phys. Rev. Lett.* **97**, 160401 (2006).